AD_____

Award Number: DAMD17-95-C-5063

TITLE: Molecular Targets for Organophosphates in the Central Nervous System

PRINCIPAL INVESTIGATOR: Edson X. Albuquerque, M.D., Ph.D.

CONTRACTING ORGANIZATION: University of Maryland at Baltimore
Baltimore, Maryland 21201

REPORT DATE: June 2004

TYPE OF REPORT: Annual

PREPARED FOR: U.S. Army Medical Research and Materiel Command
Fort Detrick, Maryland 21702-5012

DISTRIBUTION STATEMENT: Approved for Public Release;
Distribution Unlimited

The views, opinions and/or findings contained in this report are those of the author(s) and should not be construed as an official Department of the Army position, policy or decision unless so designated by other documentation.

BEST AVAILABLE COPY

20040922 042

REPORT DOCUMENTATION PAGE

Form Approved
OMB No. 074-0188

Public reporting burden for this collection of information is estimated to average 1 hour per response, including the time for reviewing instructions, searching existing data sources, gathering and maintaining the data needed, and completing and reviewing this collection of information. Send comments regarding this burden estimate or any other aspect of this collection of information, including suggestions for reducing this burden to Washington Headquarters Services, Directorate for Information Operations and Reports, 1215 Jefferson Davis Highway, Suite 1204, Arlington, VA 22202-4302, and to the Office of Management and Budget, Paperwork Reduction Project (0704-0188), Washington, DC 20503

1. AGENCY USE ONLY (Leave blank)

2. REPORT DATE
June 2004

3. REPORT TYPE AND DATES COVERED
Annual (18 May 03-18 May 04)

4. TITLE AND SUBTITLE
Molecular Targets for Organophosphates in the Central Nervous System

5. FUNDING NUMBERS
DAMD17-95-C-5063

6. AUTHOR(S)
Edson X. Albuquerque, M.D., Ph.D.

7. PERFORMING ORGANIZATION NAME(S) AND ADDRESS(ES)
University of Maryland at Baltimore
Baltimore, Maryland 21201

E-Mail: ealbuque@umaryland.edu

8. PERFORMING ORGANIZATION REPORT NUMBER

9. SPONSORING / MONITORING AGENCY NAME(S) AND ADDRESS(ES)
U.S. Army Medical Research and Materiel Command
Fort Detrick, Maryland 21702-5012

10. SPONSORING / MONITORING AGENCY REPORT NUMBER

11. SUPPLEMENTARY NOTES

12a. DISTRIBUTION / AVAILABILITY STATEMENT
Approved for Public Release; Distribution Unlimited

12b. DISTRIBUTION CODE

13. ABSTRACT (Maximum 200 Words)

No abstract provided.

14. SUBJECT TERMS
No subject terms provided.

15. NUMBER OF PAGES
23

16. PRICE CODE

17. SECURITY CLASSIFICATION OF REPORT
Unclassified

18. SECURITY CLASSIFICATION OF THIS PAGE
Unclassified

19. SECURITY CLASSIFICATION OF ABSTRACT
Unclassified

20. LIMITATION OF ABSTRACT
Unlimited

Table of Contents

Cover.....

SF 298.....

Table of Contents.....

Introduction.....3,12,13,15

Body.....3,12,13,15

Key Research Accomplishments.....

Reportable Outcomes.....5,12,13,15

Conclusions.....

References.....20

Appendices.....

SUMMARY OF PROJECT GOALS

In a continued effort to determine the actions and effects of low-level exposure to the nerve agents sarin, soman, and VX in the mammalian CNS and to help design countermeasures to treat and/or prevent such effects, we have been worked toward accomplishing the following objectives:

1. Determine whether pyridostigmine and the nicotinic APL galanthamine (also spelled galantamine) can antagonize the effects of VX, soman, and sarin on synaptic transmission in the mammalian CNS, and, if so, to elucidate the mechanism.
2. Investigate whether chronic exposure of CNS neurons to soman, VX, and sarin results in neuronal death.
    a. Determine the mechanism(s) that contribute(s) to nerve agent-induced cell death: apoptosis and/or necrosis
    b. Determine which pathways (AKT, MEK/MEK Kinase, caspases, etc.) underlie nerve-agent-induced neuronal death, in the case apoptosis is the major component of neuronal death induced by chronic exposure to low levels of sarin, soman, and VX.
    c. Investigate if neuronal death induced by chronic exposure to low levels of sarin, soman, and VX can be antagonized by galantamine
    d. Analyze the effects of pyridostigmine on neuronal viability and determine if pyridostigmine could antagonize or facilitate neuronal death induced by chronic exposure to low levels of sarin, soman, and VX.
3. Determine the effects of chronic exposure to low levels of sarin, soman, and VX on acetylcholinesterase, choline acetyltransferase, and nicotinic receptor expression in primary cultures of hippocampal neurons.
4. Investigate whether chronic exposure to low levels of sarin, soman, and VX alters KYNA levels in the rat brain.
5. Analyze whether chronic exposure to low levels of these nerve agents could alter innervation of the hippocampus by the septum in organotypic septal-hippocampal cultures, and, if so, investigate whether changes in the cholinergic system and/or in KYNA levels underlie such effects.

PROGRESS ON AIM 1:

LOW CONCENTRATIONS OF PYRIDOSTIGMINE PREVENT SOMAN-INDUCED INHIBITION OF GABAERGIC TRANSMISSION IN THE CENTRAL NERVOUS SYSTEM: INVOLVEMENT OF MUSCARINIC RECEPTORS

INTRODUCTION

In our last progress report, we described our studies that showed how soman, pyridostigmine, and galantamine on synaptic transmission in rat hippocampal slices and also described how pyridostigmine could counteract the effects of soman. Soman was shown to selectively reduce GABAergic transmission in the hippocampus, and pyridostigmine, when pre-applied could prevent the OP's effects. Here we report our detailed analysis of pyridostigmine's ability to block soman-induced reduction in GABAergic transmission, and the analysis of the underlying mechanism.

MATERIALS AND METHODS

Rat hippocampal slices. Hippocampal slices of 250-μm thickness were obtained from 15-25-day-old Sprague-Dawley rats according to the procedure described earlier (Alkondon et al., 1999). The slices were kept in a holding chamber containing artificial cerebrospinal fluid (ACSF) bubbled with 95% O_2 and 5% CO_2, at room temperature. Each slice, as needed, was transferred to a recording chamber (capacity of 2 ml) and held submerged by two nylon fibers. The recording chamber was continuously perfused with bubbled ACSF, which had the following composition (in mM): NaCl, 125; $NaHCO_3$, 25; KCl, 2.5; NaH_2PO_4, 1.25; $CaCl_2$, 2; $MgCl_2$, 1 and glucose, 25 (osmolarity ~340 mOsM).

Electrophysiological recordings. By means of the whole-cell mode of the patch-clamp technique, spontaneous or field stimulation-evoked postsynaptic currents (PSCs) were recorded from neurons of the CA1 pyramidal layer of rat hippocampal slices. Test solutions were applied to the slices through a set of coplanar-parallel glass tubes (400 μm i.d.) glued together and assembled on a motor driven system (Newport Corporation, Irvine, CA) controlled by microcomputer. The tubes were placed at a distance of approximately 100-150 μm from the slice, and the gravity-driven flow rate was adjusted to 1.0 ml/min. Each tube was connected to a different reservoir filled with test solution. Evoked PSCs were recorded following application of a supramaximal 20-60-μs electrical stimulus to afferent fibers via a bipolar electrode made of thin platinum wires (50-100-μm diameter). The stimulus was delivered by an isolated stimulator unit (Digitimer Ltd., Garden City, England) connected to a digital-to-analog interface (TL-1 DMA, Axon Instrument Inc., Foster City, CA). The platinum electrode was positioned at the Schaffer collaterals. Possible changes in series resistance were detected by applying, online, a 5-mV hyperpolarizing pulse before the test pulse.

Electrophysiological signals were recorded by means of an Axopatch 200A (Axon Instruments, Inc. CA) filtered at 2 kHz, and either stored on VCR tapes or directly sampled by a microcomputer using the pClamp6 software (Axon Instruments, Foster City, CA). Low-resistance (2-5 MΩ) electrodes were pulled from borosilicate capillary glass (World Precision Instruments, New Haven, CT) and filled with internal solution. The composition of the internal solution used for voltage-clamp recordings from neurons in the CA1 pyramidal layer was (in mM): CsCl, 80; CsF, 80; EGTA, 10; CsOH, 22.5; HEPES, 10 and QX-314, 5 (pH adjusted to 7.3 with CsOH; 340 mOsM). All experiments were performed at room temperature (20-22°C)

Data analysis. Peak amplitude, 10-90% rise time, and decay-time constant of field stimulation- evoked PSCs were determined using the pClamp6 software. Spontaneously occurring currents were analyzed using the Continuous Data Recording software (Dempster,

1989). All the analyses were made on fixed 3-min recordings. Unless otherwise stated, data are presented as mean ± S.E.M. The Student's t-test was used for pairwise comparison of results obtained in a test group and its respective control. In addition, one-way analysis of variance (ANOVA) followed by Turkey's post-hoc test was used to compare results of repeated measures and multiple groups.

Cholinesterase assay. Cholinesterase activity was measured by a two-phase radiotopic assay (Johnson and Russel, 1975) using 0.788 mM [3H]ACh chloride, which was sufficient to produce 100,000 cpm when totally hydrolyzed. The reaction (100 µl) was terminated by addition of 100 µl of a termination mixture (1 M monochloroacetic acid, 2 M NaCl, 0.5 M NaOH) to which 4 ml of scintillation mixture (10% isoamyl alcohol, 0.5% diphenyloxazole, 0.02% dimethylphenyloxazolylbenzene in toluene) was added. The hydrolyzed, acidified [3H]acetate partitioned into the organic phase and was subsequently counted. All samples were assayed in the presence of the butyrylcholinesterase inhibitor tetraisopropylpyrophosphoramide (10^{-4} M). Protein assays were performed using a micro BCA Kit (Pierce, Rockford, Il) according to the manufacturer instructions. Two sets of experiments were carried out. In one set, hippocampal slices were first perfused for 15 min with ACSF containing no drug, soman (1 nM) or PB (100 nM) and subsequently washed three times with drug-free ACSF for 1.5 min. Each slice was transferred to a microfuge tube containing 50 µl of extraction buffer (pH = 7.4; NaCl 1 M; $NaH_2PO4.H_2O$ 0.019 M; $NaHPO_4.7H_2O$ 0.081 M; Titron X-100 1%) and snap frozen. Cells within the slices were lysed by five rounds of freeze-thaw, lasting approximately 5 min, and homogenates were centrifuged at 14,000 rpm at 4°C. Cholinesterase activity measured in the supernatant was normalized to the protein contents of the pellets. In the other set of experiments, hippocampal slices were first extracted as above and cholinesterase activity was measured in the supernatants after 0, 15, 30 and 60 min' exposure to PB (100 nM).

Drugs and biological hazards. Soman (1,2,2-trimethylpropyl methylphosphonofloridate) was obtained from the U.S. Army Medical Research and Development Command (USAMRDC). Atropine sulfate, PB, 6-cyano-7-nitroquinoxaline-2,3-dione (CNQX), 2-amino-5-phosphonovaleric acid (APV), picrotoxin and 4-diphenylacetoxy-*N*-methypiperidine (4-DAMP) were purchased from Sigma Chemical Co. (St. Louis, MO). 11-[[[2-diethylamino-*O*-methyl]-1-piperidinyl]acetyl]-5,11-dihydrol-6*H*-pyridol[2,3-*b*][1,4]benzodiazepine-6-one (AFDX-116) was purchased from Tocris Cookson Inc. (Ellisville, MO). Methyllycaconitine (MLA) citrate was a gift from Prof. M. H. Benn (Department of Chemistry, University of Calgary, Alberta, Canada). Dihydro-β-erythroidine (DHβE) hydrobromide was a gift from Merck (Rahway, NJ). A 250 mM stock solution of picrotoxin was made in DMSO, and dilutions were made in the ACSF. NaOH was used to dissolve CNQX and APV (the 10 mM stock solution of CNQX had 12.5 mM NaOH and the 50 mM stock solution of APV had 0.5 M of NaOH). [3H]ACh (specific activity = 55 mCi/mmol) was obtained from Perkins Elmer Life Sciences Inc./New England Nuclear (Boston, MA)

Safe handling of organophosphates was assured according to USAMRDC's recommendations. The compounds were stored at -80°C and diluted daily in an organophosphate vapor-proof hood. All organophosphate- and/or tetrodotoxin-containing solutions were inactivated with 5% sodium hypochloride. Latex gloves and proper goggles were used throughout the experiment.

RESULTS AND DISCUSSION

EPSCs evoked by field stimulation of Schaffer collaterals were recorded from CA1 pyramidal neurons in rat hippocampal slices that were continuously perfused with ACSF containing the GABAA receptor antagonist picrotoxin (100 μM). Likewise, IPSCs evoked by field stimulation of Schaffer collaterals were recorded from CA1 pyramidal neurons in rat hippocampal slices that were continuously perfused with ACSF containing the glutamate receptor antagonists CNQX (20 μM) and APV (50 μM). As shown in Figure 1, during the recording time, the amplitudes of these synaptic currents were fairly stable.

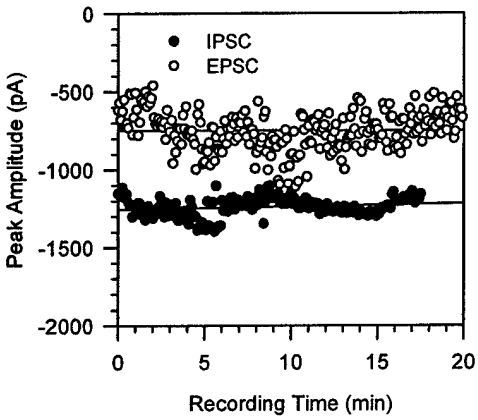

Figure 1. *Time-dependent changes in the amplitudes of EPSCs and IPSCs evoked by stimulation of the Schaffer collaterals and recorded from CA1 pyramidal neurons in rat hippocampal slices.* Plot of the amplitudes of EPSCs or IPSCs evoked by field stimulation of the Schaffer collaterals at 0.2 Hz and recorded from CA1 pyramidal neurons versus recording time. Holding potential, −60 mV.

When the hippocampal slices were perfused with ACSF containing soman (0.1-10 nM), there was a concentration-dependent reduction of the amplitude of the IPSCs evoked by stimulation of the Schaffer collaterals and recorded from CA1 pyramidal neurons (Figure 2).

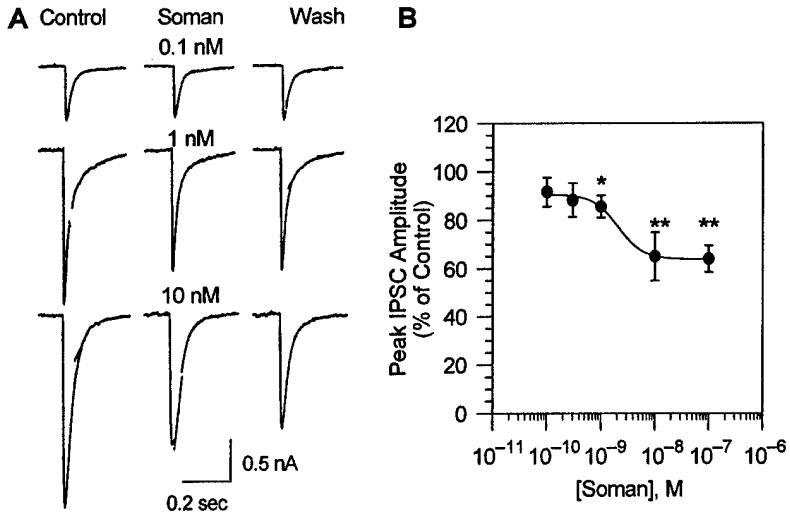

Figure 2. *Effect of soman on the amplitude of IPSCs evoked by field stimulation of the Schaffer collaterals and recorded from CA1 pyramidal neurons in rat hippocampal slices.* **A.** Representative recording samples of evoked IPSCs obtained (i) under control conditions, (ii) in the presence of 0.1, 1 or 10 nM soman, and (iii) after 10-min washing of the slices with soman-free ACSF. The neurons were exposed for 10 min to soman. All experiments were carried out in the presence of CNQX (20 μM) and APV (50 μM). Membrane potential, −60 mV. **B.** Concentration-dependent effect of soman on evoked IPSCs. Each concentration was tested on a slice that had not been previously exposed to soman. Graph and error bars represent mean and S.E.M., respectively, of results obtained from 4 neurons. According to the unpaired Student's t-test, results are significantly different from control with $p < 0.05$ (*) or $p < 0.01$ (**).

The effect of soman was selective for GABAergic transmission, because the amplitudes of EPSCs evoked by stimulation of the Schaffer collaterals and recorded from CA1 pyramidal neurons were not affected by soman at concentrations as high as 50 nM (Figure 3).

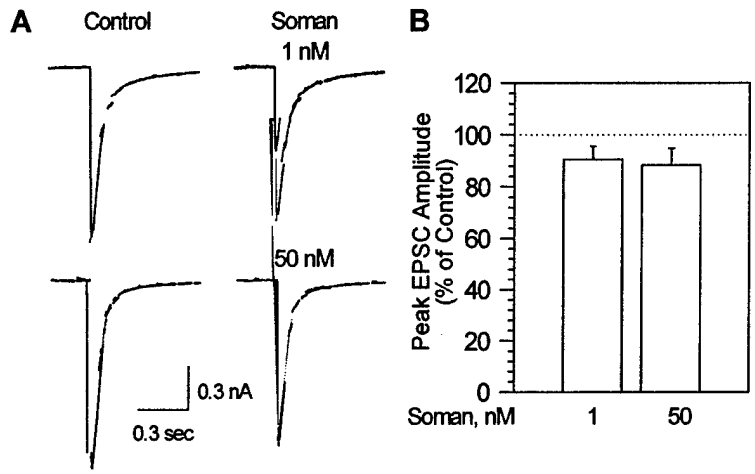

Figure 3. *Soman does not affect field sitmulation-evoked EPSCs recorded from CA1 pyramidal neurons.* **A.** Samples of evoked EPSCs recorded from neurons at -60 mV before (left traces) and during exposure to 1 or 50 nM soman (right traces). **B.** Quantitative analysis of the effect of soman on evoked EPSCs. Graph and error bars represent mean and S.E.M., respectively, of results obtained from 4 neurons.

Exposure of the hippocampal slices to soman also had a selective effect on the spontaneous, action potential-dependent GABAergic transmission between the Schaffer collaterals and CA1 pyramidal neurons. Of interest, however, soman-induced reduction of amplitude and frequency of spontenously occurring IPSCs was more pronounced when the events were recorded between successive field stimulations of the Schaffer collaterals (see Figure 4).

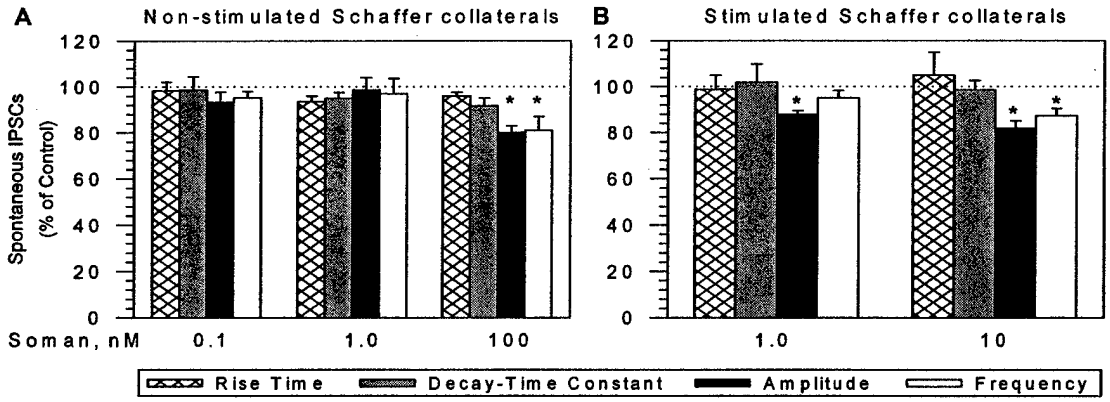

Figure 4. *Soman decreases the amplitude and frequency of spontaneously occurring IPSCs recorded from CA1 pyramidal neurons in rat hippocampal slices.* **A.** Quantitative analysis of the effects of soman on spontaneous IPSCs recorded from CA1 pyramidal neurons in slices where the Schaffer collaterals had not been field stimulated. The average rise time and decay-time constant of IPSCs recorded from neurons prior to their exposure to soman were 2.5 ± 0.55 msec and 7.5 ± 1.44 msec, respectively. **B.** Quantitative analysis of the effects of soman on spontaneous IPSCs recorded from CA1 pyramidal neurons in slices where the Schaffer collaterals were stimulated at 0.2 Hz. The average rise time and decay-time constant of IPSCs recorded under control conditions were 2.03 ± 0.39 msec and 8.16 ± 1.73 msec, respectively. Graph and error bars represent mean and S.E.M., respectively, of results obtained from 5 neurons at −60 mV. According to the unpaired Student's t-test, results are significantly different from control with $p < 0.05$ (*).

Soman-induced inhibition of GABAergic transmission in hippocampal slices was mediated exclusively by muscarinic receptors, because it could be prevented by perfusion of the slices with ACSF containing atropine (Figure 5A) and it was not affected by the nAChR antagonists methyllycaconitine (MLA) and dihydro-β-erythroidine (DHβE) (Figure 5B).

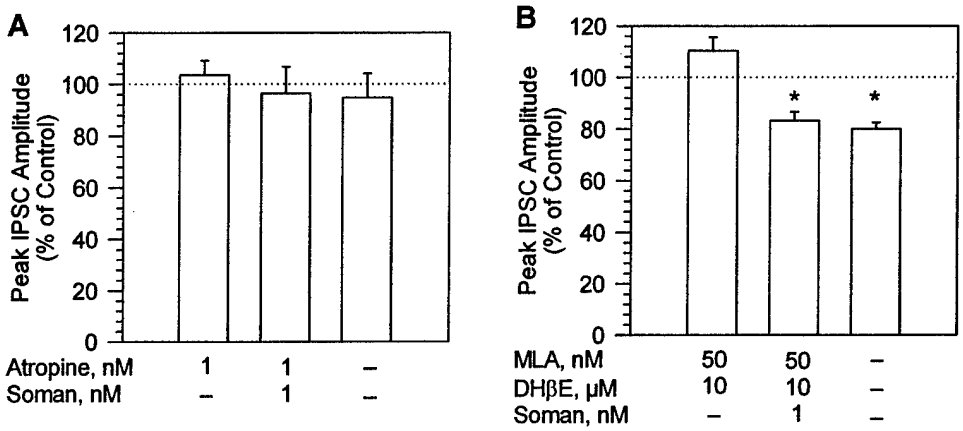

Figure 5. *Effects of the muscarinic receptor antagonist atropine and the nAChR antagonists MLA and DHβE on soman-induced inhibition of evoked IPSCs in rat hippocampal slices.* **A.** Quantitative analysis of the effect of atropine on evoked IPSCs and on soman-induced inhibition of evoked IPSCs. Evoked IPSCs were recorded from CA1 pyramidal neurons in hippocampal slices that were exposed first to atropine (1nM) for 5-8 min and subsequently to the admixture of atropine (1 nM) plus soman (1 nM) for an additional 10 min. At the end of the experiments, the preparations were washed for 10 min with drug-free ACSF. The amplitudes of events evoked at a frequency of 0.2 Hz for 3 min were averaged. The averaged amplitudes of events recorded in the presence of atropine or atropine-plus-soman and in the washing phase are expressed as percentage of the averaged amplitudes of events recorded at the same frequency for 3 min prior to exposure of the neurons to any drug. **B.** Quantitative analysis of the effect of MLA and DHβE on evoked IPSCs and on soman-induced inhibition of evoked IPSCs. Evoked IPSCs were recorded from CA1 pyramidal neurons in hippocampal slices that were exposed first to MLA (50 nM) plus DHβE (10 μM) for 5-8 min and subsequently to the admixture of the antagonists and soman (1 nM) for an additional 10 min. At the end of the experiments, the preparations were washed for 10 min with drug-free ACSF. The amplitudes of events evoked at a frequency of 0.2 Hz for 3 min were averaged. The averaged amplitudes of events recorded in the presence of drugs and in the washing phase are expressed as percentage of the averaged amplitudes of events recorded at the same frequency for 3 min under control conditions. Graph and error bars represent mean and S.E.M., respectively, of results obtained from 4 neurons at -60 mV. All experiments were carried out in the presence of CNQX and APV. According to the unpaired Student's t-test, results are significantly different from control with $p < 0.05$ (*).

In contrast to soman, pyridostigmine bromide (PB) at nanomolar concentrations increased the amplitude of IPSCs evoked by field stimulation of the Schaffer collaterals and recorded from CA1 pyramidal neurons in hippocampal slices (Figure 6A). Like soman, however, PB did not affect glutamatergic transmission in the hippocampal slices (Figure 6B). The effect of PB on GABAergic transmission was concentration dependent, being maximal at 100 nM (Figure 6C) and was completely reversible upon washing the preparations with PB-free physiological solution (Figure 6A).

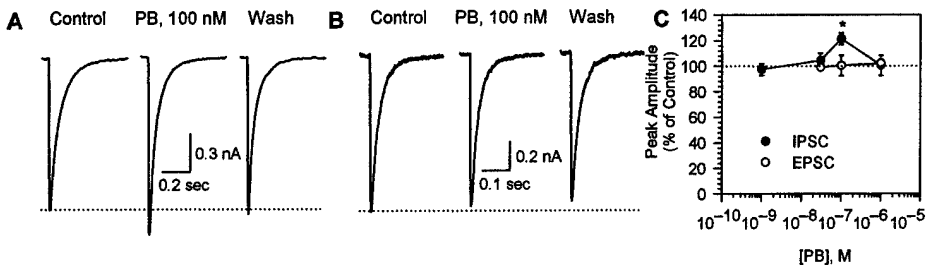

Figure 6. *PB increases the amplitude of IPSCs and does alter the amplitude of EPSCs evoked by field stimulation of the Schaffer collaterals and recorded from CA1 pyramidal neurons in rat hippocampal slices.* **A, B.** Sample recordings of evoked IPSCs (**A**) and EPSCs (**B**) obtained from two neurons under control conditions, in the presence of PB (100 nM) and after 10-min washing of the preparations with PB-free ACSF. The neurons were exposed to PB for 10 min. Evoked IPSCs were recorded in the presence of CNQX (20 μM) and APV (50 μM), and evoked EPSCs were recorded in the presence of picrotoxin (100 μM). Holding potential, −60 mV. **C.** Graph of PB concentrations vs. the amplitudes of evoked EPSCs or IPSCs normalized to control conditions. The amplitudes of EPSCs or IPSCs evoked at a frequency of 0.2 Hz for 3 min were averaged. The averaged amplitudes of events recorded in the presence of PB are expressed as percentage of the averaged amplitudes of events recorded at the same frequency for 3 min under control conditions. Graph and error bars represent mean and S.E.M., respectively, of results obtained from 4 neurons. According to the unpaired Student's t-test, results are different from control with $p < 0.05$ (*).

The facilitatory effect of PB on field stimulation-evoked GABAergic transmission in the hippocampus was mediated primarily by muscarinic receptors, as it was selectively blocked by 1 nM atropine (Figure 7).

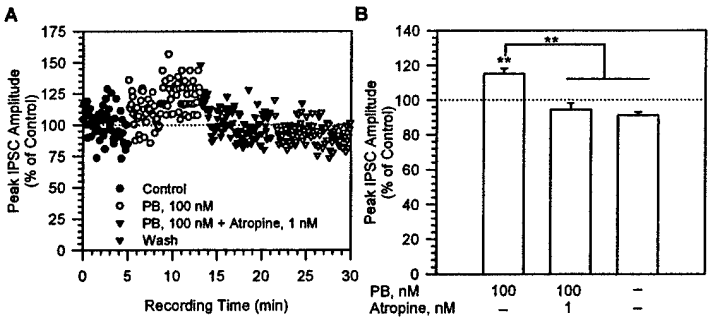

Figure 7. *Atropine blocks PB-induced potentiation of IPSCs evoked by field stimulation of the Schaffer collaterals and recorded from CA1 pyramidal neurons.* **A.** Graph of the amplitudes of IPSCs evoked at 0.2 Hz and recorded from a CA1 pyramidal neuron: (i) under control condition, (ii) in the presence of 100 nM PB, (iii) in the presence of 100 nM PB and 1 nM atropine, and (iv) during the wash-out with drug-free ACSF. **B.** Quantitative analysis of the effects of 1 nM atropine on PB-induced potentiation of evoked IPSCs. The amplitudes of IPSCs evoked at a frequency of 0.2 Hz for 3 min were averaged. The averaged amplitudes of events recorded from a given neuron in the presence of PB or atropine-plus-PB and during the washing phase are expressed as percentage of the averaged amplitudes of events recorded at the same frequency for 3 min under control conditions. Graph and error bars represent mean and S.E.M., respectively, of results obtained from 5 neurons at -60 mV. All experiments were carried out in the presence of the glutamate receptor antagonists CNQX (20 μM) and APV (50 μM). According to the ANOVA test, peak amplitudes of IPSCs recorded in the presence of PB prior to exposure of the neurons to 1 nM are significantly different from control with $p < 0.01$ (**). Finally, amplitudes of events recorded during exposure of neurons to PB-plus-atropine and after removal of both drugs were significantly different from those recorded in the presence of PB alone with $p < 0.01$ (**).

In addition to increasing the amplitude of field stimulation-evoked IPSCs, PB at nanomolar concentrations also increases the frequency and amplitude of spontaneous IPSCs recorded from CA1 pyramidal neurons and these effects are also blocked by the muscarinic receptor antagonist atropine (Figure 8).

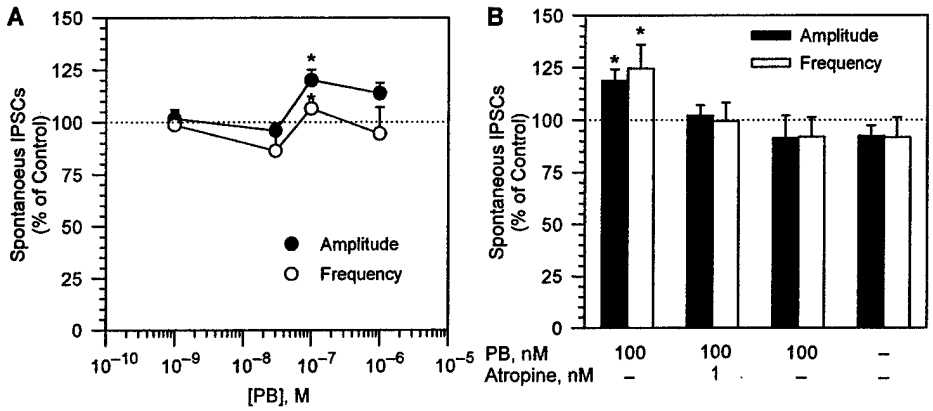

Figure 8. *Atropine blocks the effects of PB on spontaneous IPSCs recorded from CA1 pyramidal neurons in hippocampal slices where the Schaffer collaterals were stimulated at 0.2 Hz.* **A.** Analyses of the effects of PB on the amplitude and frequency of spontaneous IPSCs. The frequency and average amplitude of IPSCs recorded for 3 min in the presence of PB are expressed as percentage of the frequency and average amplitude of events recorded under control condition. Points and error bars represent mean and S.E.M., respectively, of results obtained from 4 neurons. Results are significantly different from those obtained under control conditions: *, $p < 0.05$ according to the unpaired Student's t-test. **B.** Analyses of the effects of atropine on PB-induced increase in the amplitude and frequency of spontaneous IPSCs. The neurons were first exposed to PB (100 nM) for 5–8 min and subsequently to PB (100 nM)-plus-atropine (1 nM). Following this treatment, the neurons were perfused for 10 min with ACSF containing only PB and for an additional 10 min with ACSF containing no atropine or PB. The frequency and average amplitude of IPSCs recorded for 3 min under each experimental condition are expressed as percentage of the frequency and average amplitude of events recorded under control condition. Graph and error bars represent mean and S.E.M., respectively, of results obtained from 4 neurons. Results were significantly different from those obtained under control conditions: *, $p < 0.05$ according to the unpaired Student's t-test.

In an attempt to define pharmacologically the muscarinic receptor subtypes underlying the effects of PB and soman on GABAergic transmission in the rat hippocampus, the m3 receptor-preferring antagonist 4-DAMP and the m2 receptor-preferring antagonist AFDX-116 were used.

Evoked IPSCs were recorded from CA1 pyramidal neurons in hippocampal slices that were exposed first to 4-DAMP (100 nM) for 5–8 min and subsequently to the admixture of 4-DAMP (100 nM) plus soman (1 nM) or PB (100 nM) for an additional 10 min. The same protocol was carried out using AFDX-116 instead of 4-DAMP. At the end of the experiments, the preparations were washed for 10 min with drug-free ACSF. The m2 receptor-preferring antagonist AFDX-116 prevented soman from inhibiting GABAergic transmission in the hippocampus, whereas the m3 receptor-preferring antagonist 4-DAMP was unable to affect the inhibitory effect of soman on GABAergic transmission (Figure 9A). In contrast, PB-induced potentiation of GABAergic transmission in the hippocampus was selectively prevented by 4-DAMP and was not altered by AFDX-116 (Figure 9B).

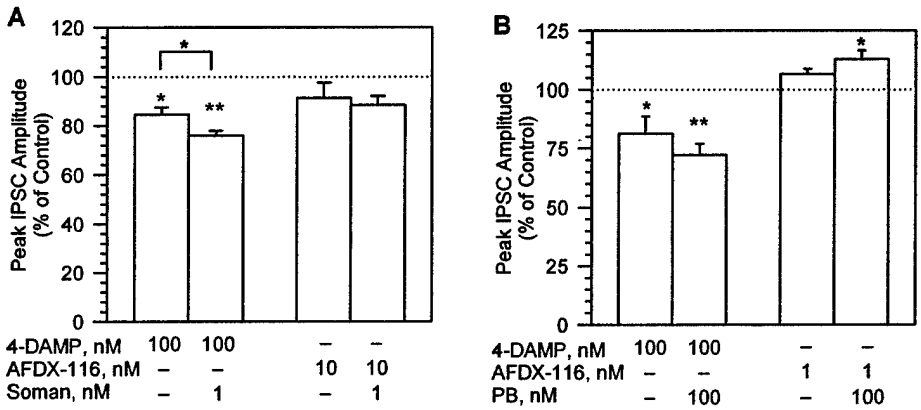

Figure 9. *Effects of AFDX-116 and 4-DAMP on soman-induced inhibition and PB-induced potentiation of evoked GABAergic transmission in hippocampal slices.* **A.** Analysis of the effects of the m3 receptor-preferring antagonist 4-DAMP and of the m2 receptor-preferring antagonist AFDX-116 on evoked IPSCs and on soman-induced inhibition of evoked IPSCs. The amplitudes of events evoked at a frequency of 0.2 Hz for 3 min were averaged. The averaged amplitudes of events recorded in the presence of a muscarinic receptor antagonist or that antagonist-plus-soman are expressed as percentage of the averaged amplitudes of events recorded at the same frequency for 3 min prior to exposure of the neurons to any drug. Each graph and error bar represents mean and S.E.M. of results obtained from 3–6 experiments. The amplitudes of currents recorded in the presence of 4-DAMP or 4-DAMP-plus-soman were significantly smaller than those recorded under control conditions: *, $p < 0.05$ and **, $p < 0.01$ according to the ANOVA test. In addition, the amplitudes of events recorded in the presence of 4-DAMP-plus-soman were significantly different from those recorded in the presence of 4-DAMP: *, $p < 0.05$ according to the ANOVA test. **B.** Quantitative analysis of the effects of the m3 receptor-preferring antagonist 4-DAMP and of the m2 receptor-preferring antagonist AFDX-116 on evoked IPSCs and on PB-induced potentiation of evoked IPSCs. The analysis is similar to that described in A. Each graph and error bar represent mean and S.E.M., respectively, of results obtained from 3–6 experiments. Amplitudes of events recorded in the presence of 4-DAMP, 4-DAMP-plus-PB, and AFDX-116-plus-PB were significantly different from those recorded under control conditions: *, $p < 0.05$; ** $p < 0.01$ according to the ANOVA test.

To determine how PB could affect soman-induced inhibition of GABAergic transmission in the hippocampus, two sets of experiments were performed. In one set of experiments, IPSCs were recorded from hippocampal slices that were exposed first to PB (100 nM), subsequently to soman (1, 3 or 10 nM) plus PB (100 nM) and finally to PB alone. In the other, IPSCs were recorded from neurons that were exposed first to PB (300 nM) and subsequently to PB (300 nM) plus soman (3 or 10 nM). Each perfusion lasted 5–8 min. The potentiating effect that 100 nM PB had on GABAergic transmission counteracted the inhibition induced by 1 nM soman. (Figure 10A and B). Of interest, the inhibitory effect of soman on evoked IPSCs was unaltered when hippocampal slices were first exposed to soman (1 nM) and subsequently to soman (1 nM)-plus-PB (100 nM) (Figure 10C).

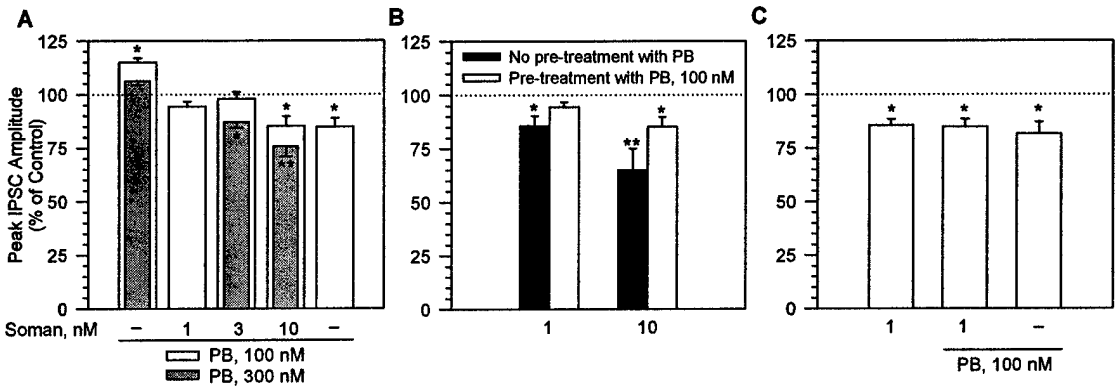

Figure 10. *Pre-exposure of the hippocampal slices to 100 nM PB masks the inhibitory effect of soman on evoked IPSCs.* **A.** Quantitative analyses of the effects of soman on evoked IPSCs recorded in the continuous presence of 100 nM or 300 nM PB. IPSCs were recorded from hippocampal slices that were exposed first to PB (100 nM), subsequently to soman (1, 3 or 10 nM) plus PB (100 nM or 300 nM) and finally to PB alone. Each perfusion lasted 5–8 min. The amplitudes of IPSCs evoked at a frequency of 0.2 Hz for 3 min were averaged. The averaged amplitudes of events recorded from a given neuron in the presence of the test compounds are expressed as percentage of the averaged amplitudes of events recorded at the same frequency for 3 min under control conditions. Graph and error bars represent mean and S.E.M., respectively, of results obtained from 3 neurons. **B.** Comparison of the effects of 1 and 10 nM soman on evoked IPSCs recorded from slices that were not pre-exposed to 100 nM PB and from slices that had been pre-exposed for 5–8 min to 100 nM PB. Data were extracted from Figs. 2B and 10A to allow mutual comparison. **C.** The inhibitory effect of soman on evoked IPSCs was unaltered when hippocampal slices were first exposed to soman (1 nM) and subsequently to soman (1 nM)-plus-PB (100 nM). The depression of the IPSCs remained after 10-min washing of the preparations with drug-free ACSF solution for at least 10 min. Analyses of the results were done according to the protocol described in **A.** Graph and error bars represent mean and S.E.M., respectively, of results obtained from 4 neurons. All experiments were carried out in the presence of CNQX (20 μM) and APV (50 μM). Holding potential, -60 mV. Wherever indicated in the graphs of panels **A**, **B** and **C**, amplitudes of events recorded in the presence of a given drug were significantly different from those of events recorded under control conditions: *, $p < 0.05$ and **, $p < 0.01$, according to the unpaired Student's t-test.

Likewise, soman (1 nM)-induced reduction of the frequency and amplitude of spontaneous IPSCs recorded from CA1 pyramidal neurons was prevented by pre-exposure of the hippocampal slices to 100 nM PB (Figure 11).

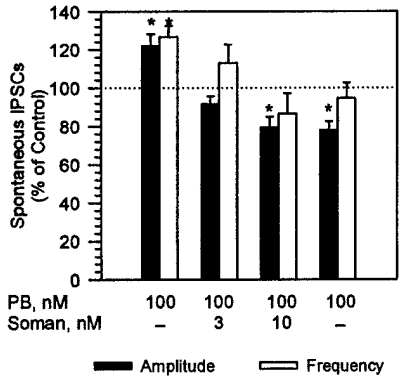

Figure 11. *Pre-exposure of the hippocampal slices to 100 nM PB masks the inhibitory effect of soman on spontaneous IPSCs recorded from CA1 neurons in hippocampal slices where the Schaffer collaterals were stimulated at 0.2 Hz.* Quantitative analyses of spontaneous IPSCs recorded from hippocampal slices exposed first to 100 nM PB and subsequently to soman (3 and 10 nM)-plus-PB (100 nM) and PB (100 nM) alone. Each perfusion lasted 5–8 min. Results obtained during a given treatment were significantly different from those obtained under control conditions: *, $p < 0.05$ according to the unpaired Student's t-test.

SUMMARY AND RELEVANCE OF THE STUDIES WITH PYRIDOSTIGMINE AND SOMAN
Potentiation of GABAergic transmission by 100 nM PB functionally antagonized soman-induced inhibition of GABAergic transmission, but only when hippocampal slices were pre-treated with PB. We showed further that, acting via m3 receptors present on GABAergic neurons, PB at 100 nM effectively prevents inhibition of GABAergic transmission induced by the interactions of soman with m2 receptors located on GABAergic neurons. Therefore, PB, acting via m3 receptors, can effectively counteract effects arising from the interactions of soman with m2 receptors in the brain.

STUDY OF THE EFFECTS OF A GALANTAMINE METABOLITE THAT IS DEVOID OF ANTICHOLINESTERASE ACTIVITY ON NICOTINIC RECEPTOR ACTIVITY IN THE HIPPOCAMPUS

INTRODUCTION
In consideration of galantamine as a potential agent to prevent/counteract the effects of OPs, the availability of a structural analogs of galantamine, a metabolite that has different properties, was intriguing. Galantaminone, one of the major metabolites of galantamine, is approximately 130-fold less potent than galantamine in inhibiting cholinesterase (Eur J Clin Pharmacol 39:603, 1990). To this end, we decided to study the effects of this metabolite on nAChR activity and to compare them to galantamine.

MATERIALS AND METHODS
The whole-cell mode of the patch-clamp technique was used to record α7 nAChR-mediated currents evoked by U-tube application of choline (1 mM) to cultured hippocampal neurons before, during and after their exposure to various concentrations of (±)galantaminone or (-) galantaminone.HBr.

RESULTS AND DISCUSSION
In the range of 1 nM to 1 μM, (−)galantaminone.HBr and (±) galantaminone were devoid of any significant effect on α7 nAChRs. At clinically used doses of galantamine, plasma concentrations of galantaminone are in the low nanomolar range [Clin Pharmacol Ther 50:420, 1991]. The present results demonstrate that, at clinically relevant concentrations, galantaminone does not affect α7 nAChR activity and suggest that this metabolite is unlike to contribute to the clinical effectiveness of galantamine. The lack of any significant effect of the galantaminone on α7 AChR activity in the hippocampus also makes it unlikely that the metabolite will figure prominently in any strategy to use galantamine to counteract nerve agent toxicity or will explain any effectiveness of galantamine itself.

PROGRESS ON AIM 2:

EFFECTS OF PYRIDOSTIGMINE, GALANTAMINE AND LOW DOSES OF NERVE AGENTS ON NEURONAL SURVIVAL IN THE CNS

INTRODUCTION

To understand the neurological effects of galantamine, pyridostigmine and nerve agents, it will be critical to determine: (i) whether the pro- and anti-apoptotic effects of these compounds are cell-type specific; (ii) the mechanisms of action underlying the pro- and anti-apoptotic effects of these compounds; and (iii) the ability of galantamine to antagonize nerve agent-induced neurotoxicity. Thus, the first part of this study was designed to determine whether galantamine (1 μM) could protect primary hippocampal cultures from degeneration induced by either the β-amyloid peptide or the protein kinase inhibitor staurosporine (STS, 100 nM) and, if so, by what mechanism. This information would lay the groundwork for further studies on the ability of galantamine to protect against brain damage caused by nerve agents.

MATERIALS AND METHODS

Primary hippocampal cultures were prepared according to the procedure described in Alkondon and Albuquerque, 1993. In the present study, cultures were used 10 days after plating the cells dissociated from the hippocampi of 18-day-old rat fetuses.

RESULTS AND DISCUSSION

Pre-exposure of hippocampal cultures to galantamine reduced the neuronal death induced by the β-amyloid peptide Aβ1-42 (Figure 12). Likewise, STS-induced apoptosis was lower in cultures that were pre- or co-treated with galantamine. However, STS-induced apoptosis was unaffected by post-treatment of the cultures with galantamine. Western blot analysis of the primary hippocampal cultures also revealed that the extracellular signal-regulated kinase (ERK), which controls cell viability in various systems, was activated after 24-h exposure to galantamine (1 μM). Thus, the neuroprotective action of galantamine at clinically relevant concentrations involves activation of ERK and can contribute to the therapeutic effectiveness of the drug in AD, particularly at early stages of the disease.

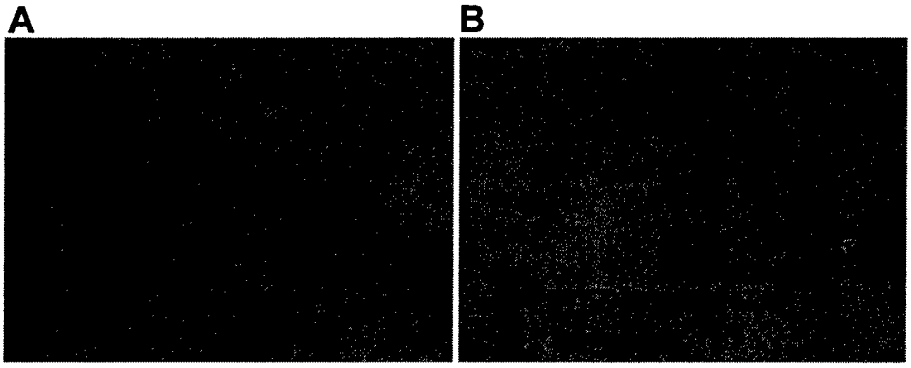

Figure 12. Effects of galantamine on Aβ1-42-induced degeneration in primary hippocampal cultures. A. TUNEL analysis of cultured hippocampal neurons that were exposed for 24 h to aggregated β-AP1-42 (10 μM). **B.** TUNEL analysis of cultured hippocampal neurons that were exposed for 24 h to galantamine (1 μM) and subsequently for an additional 24 h to the admixture of galantamine and β-AP1-42. Notice that the number of TUNEL-positive cells in the primary cultures that were exposed to galantamine prior to their exposure to Aβ1-42 was lower than the number of TUNEL-positive cells in cultures that were not pre-treated with galantamine. Calibration, 100 μm.

PROGRESS ON AIM 3

EFFECTS OF EXPOSURE TO LOW LEVELS OF SOMAN, SARIN, AND VX ALTERS CHOLINERGIC PARAMETERS, INCLUDING LEVELS OF nAChRS, CHOLINE ACETYLTRANSFERASE, ACETYLCHOLINESTERASE, AND KYNURENIC ACID (AN ENDOGENOUS METABOLITE RECENTLY IDENTIFIED AS AN ENDOGENOUS NON-COMPETITIVE ANTAGONIST OF A7 NACHRS)

Recent studies have indicated that acute exposure of the mammalian central nervous system to low levels of sarin not only decreases cholinesterase activity, but also increases choline acetyltransferase activity and causes an initial reduction followed by a sustained increase in nicotinic and muscarinic receptor expression. These effects were selectively observed in certain areas of the brain, particularly in the cortex, midbrain, and brain stem (Khan et al., 2000). There is no data available regarding the effects of VX and soman on these parameters, and much less is known regarding the effects of chronic exposure to low levels of VX, soman, or sarin on cholinergic function in the mammalian CNS.

A recent study from our laboratory has shown that the tryptophan metabolite kynurenic acid (KYNA) acts as a selective, non-competitive antagonist at α7 nAChRs and suggested that this substance may function as an endogenous modulator of α7 nAChR activity. KYNA has neuroprotective and neuroinhibitory properties that have been attributed to its action as a competitive antagonist at the glycine site on *N*-methyl-D-aspartate (NMDA) receptors (Stone, 1993; Parsons et al., 1997). However, high micromolar concentrations of KYNA are often needed to block NMDA receptor function (Stone, 1993). Considering that KYNA levels in brains of non-primates and primates (including humans) range from low nanomolar to low micromolar (Moroni et al., 1988; Turski et al., 1988), it is uncertain whether endogenous KYNA levels are sufficiently high to block NMDA receptor activity (Scharfman et al., 1999; Urenjak and Obrenovitch, 2000). It is more likely that the actions of KYNA in the nicotinic cholinergic system account for its neurological effects (Hilmas et al., 2001).

Cerebral KYNA levels are increased in patients with Alzheimer's disease (AD; Baran et al., 1999), Down Syndrome (DS; Baran et al., 1996), and schizophrenia (Schwarcz et al., in press), and decreased in patients with end-stage Parkinson's disease (PD; Ogawa et al., 1992) and Huntington's disease (HD, Beal et al., 1990). Manipulations of brain levels of KYNA in laboratory animals supported the concept that increased KYNA levels are neuroprotective and anticonvulsant, whereas decreased levels of the metabolite increase neuronal vulnerability (Pellicciari et al., 1994; Poeggeler et al., 1998; Cozzi et al., 1999). Thus, it is possible that the neuropathological effects of chronic exposure to low levels of sarin, soman, and VX could be attributed, at least in part, to changes in the nicotinic cholinergic system activity due to alterations in brain KYNA levels.

PROGRESS ON AIM 4

CHRONIC EXPOSURE TO ORGANOPHOSPHATES TARGETS SPINES ON THE BASAL DENDRITES OF THE CA1 HIPPOCAMPAL PYRAMIDAL NEURONS: IMPLICATIONS TO COGNITIVE DISORDERS

INTRODUCTION

Co-culturing of septal tissue along with hippocampal neurons results in changes in the pattern of dendritic and axonal arborization of CA1 pyramidal neurons. Thus it appears that cholinergic innervation of the hippocampus has a major impact on the development of the hippocampal neurocircuitry. As changes in the neurocircuitry of the hippocampus under underlie epileptic seizures in several experimental models, and as the OPs are known to be pro-convulsant agents, it is important to investigate the influence of low levels of OPs on septum-induced changes in the axonal and dendritic development.

Studies with another organophospate compound led us to what is probably a much more important aspect of the effects of this class of drugs on axonal and dendritic development and cytoarchitecture. Before carrying out these studies using the nerve agents, we used a readily available agent, parathion. Parathion through its oxidized active metabolite paraoxon is one of the most potent cholinesterase (ChE) inhibitor and toxic organophosphate (OP) compounds. Although banned in some developed countries including U.S., the increasing worldwide use of parathion led the World Health Organization to recognize this OP as the prime cause of accidental and occupational intoxication and fatalities. Chronic exposure to anti-ChE agents is likely to affect selectively certain brain areas leading to delayed neurological disorders. During development in animal models, cortical cholinergic disruption produces deficits in axogenesis, synaptogenesis and especially at the dendritic spines that will persist into adulthood with an impact on neuronal plasticity, long-term potentiation (LTP) and memory consolidation.

MATERIALS AND METHODS

Here we studied the effects of repetitive exposure of 8 to 20 days postnatal Wistar rats, (P8-P20) to subcutaneous daily injections of low doses of paraoxon (0.1, 0.15 and 0.2 mg/kg) during the period of significant development of cholinergic system. Pyramidal neurons of the hippocampal CA1 region, as well as the overall cytoarchitecture of the hippocampal strata, were correlated with ChE levels and hippocampal staining and with choline acetyltransferase (ChAT) immunohistochemistry. At P21, 24 h after the last injection, the brain were processed for morphological and histochemical staining assays. A group of animals was allowed to recover for 7 days from the OP exposure, the assays performed at P28 and the results compared to those obtained from another group that continued to receive paraoxon up to P27.

RESULTS AND DISCUSSION

Sub-chronic treatment of rats with paraoxon reduced the rate of body weight gain (Figure 13).

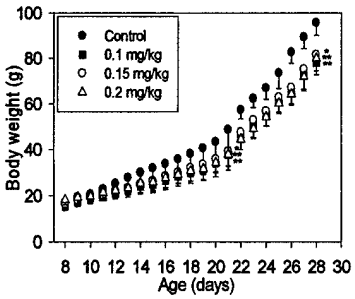

Figure 13. Chronic paraoxon exposure decreases the rate of animal development. Body weight was measured daily from P8 to P28, before the animals were injected with either peanut oil (control) or different concentrations of paraoxon. At P21, a 13, 14 and 27% decrease in body weight compared to control (filled circle) was found in animals exposed to 0.1 (filled square), 0.15 (open circle) and 0.2 (open triangle) mg/kg paraoxon, respectively. At P28, similar values of 14, 16 and 28% were found with increasing paraoxon concentrations. Differences were statistically significant at P21 and P28 (ANOVA and Dunnet's test,** $p < 0.01$ and * $p < 0.05$).

Total brain ChE activity progressively decreased up to 40% of control by day 21 (Figure 14). At P28, ChE levels were further decreased to 39, 33 and 30% of control in animals exposed to 0.1, 0.15 and 0.2 mg/kg, respectively, and the ChE recovery, although significant, was not complete, reaching 75, 74 and 66% of control for the three increasing doses. ChE staining was reduced in all hippocampal and dentate gyrus regions.

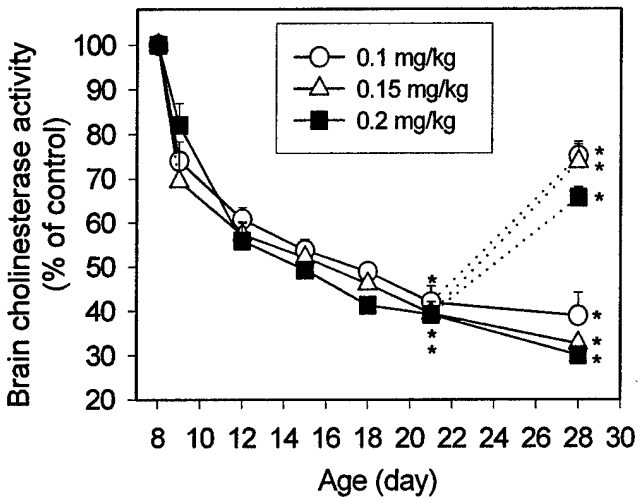

Figure 14. Decrease of brain ChE activity during chronic paraoxon treatment. Brain ChE activity is expressed as percentage of control *versus* days of age. ChE activity was assayed each 3 days, 24 hours after the last paraoxon injection. Animals exposed daily to 0.1 (open circle); 0.15 (open triangle) or 0.2 mg/kg (filled square) showed progressive ChE inhibition that reached 60% of control at P21 (n = 4, for each group) and 70% at P28 (n = 3). Animals receiving the last injection at P20 and examined at P28 showed significant recovery in ChE activity (dotted lines, n = 4) when compared to those continuously treated (ANOVA and SNK test, $p < 0.01$), but were still significantly below control values (ANOVA and Dunnet's test with 8 or 12 DF,* $p < 0.01$).

Cresil violet staining showed neither cytoarchitectural changes nor signs of cell body degeneration as judged by the absence of pyknotic hyperchromatic neurons. To evaluate the effects of paraoxon on neuronal structure, CA1 pyramidal neurons were filled with Lucifer Yellow (Figure 15).

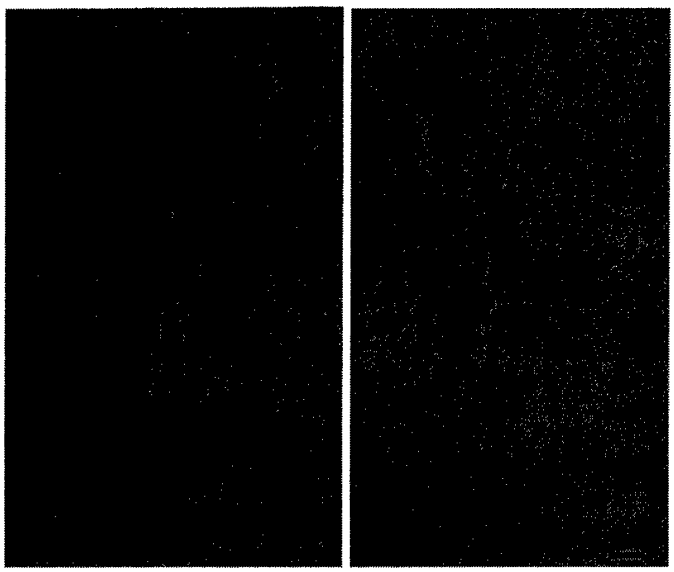

Figure 15. Photomicrographs of Lucifer yellow-filled CA1 pyramidal neurons at P21. Pyramidal neurons from control (A) and paraoxon (0.2 mg/kg)-injected (B) animals were filled with LY and subsequently treated with peroxidase-conjugated anti-LY antibody. Cells from the two experimental groups showed a high degree of morphological homogeneity, and paraoxon did not produce any noticeable alterations. Calibration bar: 50 µm.

Paraoxon selectively decreased the spine density on the basal, but not on the secondary apical dendrites (Figure 16).

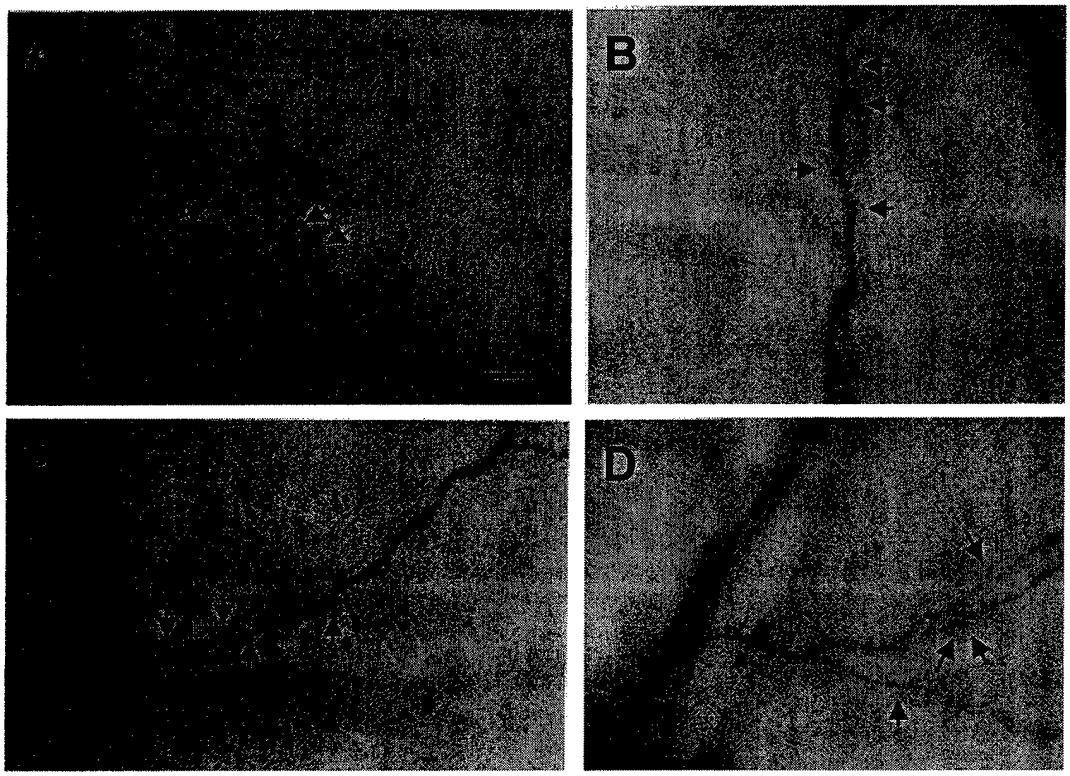

Figure 16. ***Paraoxon selectively reduces the spine density on the basal dendrites of CA1 pyramidal neurons at P21.*** Photomicrographs show basal and apical dendrites of pyramidal neurons filled with LY and subsequently treated with horseradish-conjugated anti-LY antibodies. A and C panels illustrate the dendritic spines of the basal tree of pyramidal neurons from control rats and from rats after treatment with 0.2 mg/kg paraoxon, respectively. The spines (indicated by the arrows), which appeared in great number on control neurons, were much fewer in number and appeared scattered along the dendrites of cells from paraoxon-treated animals. In contrast, the density of the dendritic spines on the secondary apical tree of pyramidal neurons from the control (B) and paraoxon-treated (D) animals showed no difference. Calibration bar: 5 μm.

In contrast, dendritic length and number of intersections and bifurcations of both basal and apical trees of CA1 pyramidal neurons were not affected by treatment of the animals with paraoxon (Figure 17). In addition, paraoxon decreased ChE activity in the hippocampus (Figure 18) without affecting ChAT activity (Figure 19) or the gross morphology of the pyramidal cell layer (Figure 20).

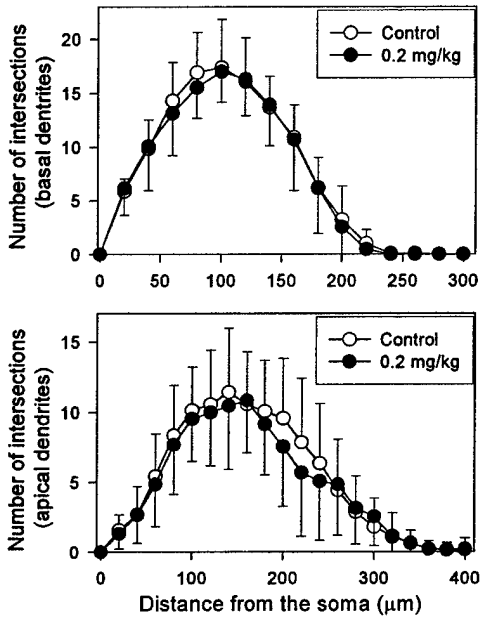

Figure 17. Paraoxon does not alter the dendritic branching pattern of CA1 pyramidal neurons. Sholl plots were used to describe the arborization pattern of the basal (top graph) and apical (bottom graph) dendrites at P21. The number of intersections made by the dendritic branches in cells from control (open symbols) and in 0.2 mg/kg paraoxon-treated (filled symbols) animals were plotted against the distance from the soma. The number of intersections of the basal or apical dendrites was counted within concentric circles spaced at 20-μm intervals from the center of the soma, and showed no differences between the two experimental groups. The points represent the mean ± S.D. of the mean of values for 14 neurons from control and 13 neurons from paraoxon-treated animals (4 animals for each group).

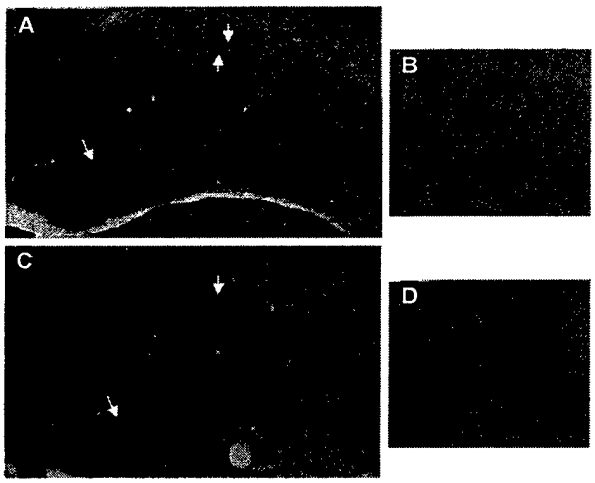

Figure 18. Paraoxon decreases cholinesterase staining in the hippocampus and dentate gyrus. In control slices (A), the AChE-positive fibers appeared concentrated in two bands, above and below the CA1 pyramidal layer (indicated by the arrows), and in the molecular layer of the dentate gyrus. In slices from animals treated with 0.2 mg/kg paraoxon (C), these bands in the Ammon's Horn were absent and the staining was much attenuated in the molecular layer of the dentate gyrus. Note the intense staining of the AChE-positive fibers in the detailed view of the control (B) as compared to paraoxon-treated slices (D). Calibration bars: 200 μm (A,C) and 12 μm (B,D).

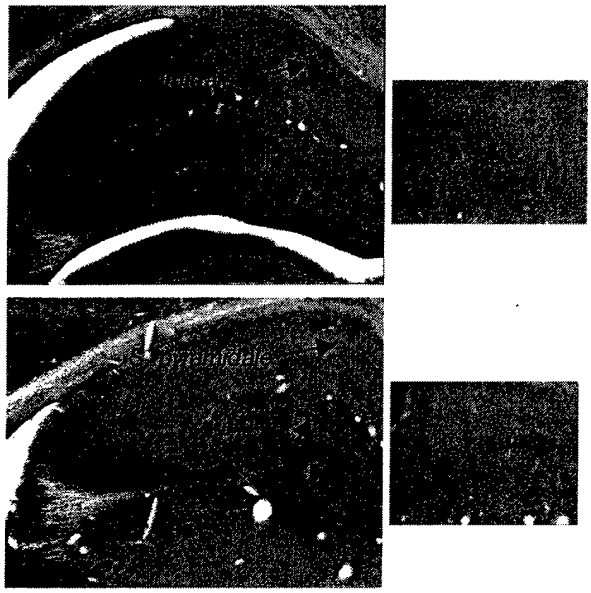

Figure 19. Paraoxon does not alter choline acetyltransferase staining in the hippocampus and dentate gyrus. ChAT immunohistochemistry of slices from control (top) and 0.2 mg/kg paraoxon-treated (bottom) animals shows positive staining throughout the hippocampus and dentate gyrus. A more intense staining was present at the border of the stratum pyramidale (see the detailed view, right panels) and at the internal molecular layer of the dentate gyrus (arrows). Calibration: 200 μM (left panels) and 12 μM (right panels).

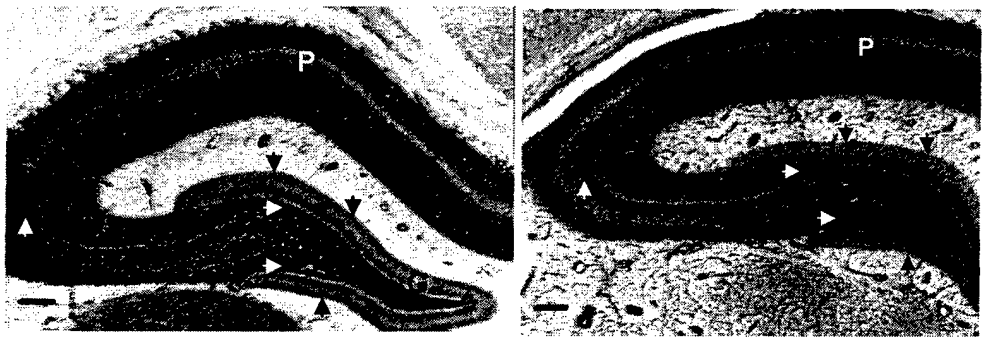

Figure 20. Timm staining of hippocampus and dentate gyrus. Pyramidal (P) and granular (G) cell layers (blue stain), the dentate gyrus mossy fibers (white arrows) and the associational/commissural fibers of the dentate gyrus (black arrows) and of the Ammon Horn (brown stain) are shown in Timm-stained slices. At P21, slices from control (top) and 0.2 mg/kg paraoxon-treated (bottom) animals showed no difference. Calibration bar: 200 μm.

Thus, chronic exposure to low doses of paraoxon during a period of cholinergic system development, despite the overall reduction of brain ChE levels, selectively affected the basal dendrite spine density of the pyramidal neurons. This fine hippocampal alteration with serious developmental consequences to cognition and other brain functions occurred in the absence of overt cholinergic toxic signs, which serves as an alert for the insidiousness of OPs when present in a repetitive low-dose scheme. These studies are very relevant to development of antidotal and/or preventative strategies using pyridostigmine and galantamine. As protection studies continue, it will be important to determine whether this damage to the fine architecture of the brain will be prevented.

RELEVANT PUBLICATIONS FROM DR. ALBUQUERQUE'S LAB SINCE THE LAST PROGRESS REPORT

MANUSCRIPTS

1. Santos, M.D., Alkondon, M., Pereira, E.F.R., Aracava, Y., Eisenberg, H.M., Maelicke, A., and Albuquerque, E.X. The nicotinic allosteric potentiating ligand galantamine facilitates synaptic transmission in the mammalian central nervous system. Mol. Pharmacol. 61:1222-1234, 2002.

2. Santos, M.D., Pereira, E.F.R., Aracava, Y., Castro, N.G., Fawcett, W.P., Randall, W.R., nad Albuquerque, E.X. Low concentrations of pyridostigmine prevent soman-induced inhibition of GABAergic transmission in the central nervous system: Involvement of muscarinic receptors. J. Pharmacol. Exp. Ther. 304:254-265, 2003.

3. Samochocki, M., Höffle, A., Fehrenbacher, A., Jostock, R., Ludwig, J., Christner, C., Radina, M., Zerlin, M., Ullmer, C., Pereira, E.F.R., Fels, G., Lübbert, H., Albuquerque, E.X., and Maelicke, A. Galantamine is an allosterically potentiating ligand of neuronal nicotinic but not of muscarinic acetylcholine receptors. J. Pharmacol. Exp. Ther. 305:1024-1036, 2003.

4. Alkondon, M., Pereira, E.F.R., and Albuquerque. NMDA and AMPA receptors contribute to the nicotinic cholinergic excitation of CA1 interneurons in the rat hippocampus. J. Neurophysiol. 90:1613-1625, 2003.

5. Santos, H.R., Cintra, W.M., Aracava, Y., Maciel, C.M., Castro, N.G., and Albuquerque, E.X. Spine density and dendritic branching pattern of hippocampal CA1 pyramidal neurons in neonatal rats chronically exposed to the organophosphate paraoxon. J. Neurotoxicol. 25:481-494, 2004.

6. Alkondon, M., Pereira, E.F.R., Yu, P., Arruda, E.Z., Almeida, E.F., Guidetti, P., Fawcett, W.P., Sapko, M.T., Randall, W.R., Schwarcz, R., Tagle, D.A., and Albuquerque, E.X. Targeted deletion of the kynurenine aminotransferase II gene reveals a critical role of engodenous kynurenic acid in the regulation of synaptic transmission via α7 nicotinic receptors in the hippocampus. J. Neurosci. 24:4635-4648, 2004.

7. Aracava, Y., Pereira, E.F.R., Maelicke, A., and Albuquerque, E.X. α7 nicotinic receptors are blocked more potently than NMDA receptors by clinically relevant concentrations of memantine: Implications for treatment of Alzheimer's disease. Mol. Pharmacol. (To be Submitted).

8. Camara, A.L., Pereira, E.F.R., Alkondon, M., Randall, W.R., Castro, N.G., and Albuquerque, E.X. Septal innervation of the hippocampus regulates expression of α7 nicotinic receptors in CA1 and CA3 pyramidal neurons. I. Neuron (To be Submitted).

9. Popa, R., Pereira, E.F.R., Aracava, Y., and Albuquerque. Galantaminone and galantamine n-butylcarbamate: candidates for the treatment of Alzheimer's disease. J. Pharmacol. Exp. Ther. (To be Submitted)

10. Alkondon, M., and Albuquerque, E.X. Two in vivo nicotine injections in less than a day differentially upregulate functional nicotinic acetylcholine receptors in rat hippocampal slices: role of receptor inactivation. Mol. Pharmacol. (To be Submitted).

11. Rassoulpour, A., Wu, H.-Q., Albuquerque, E.X., Schwarcz, R. Prolonged nicotine administration results in biphasic, brain-specific changes in kynurenate levels in the rat. Neuropspychopharmacology (Submitted).

PRESENTATIONS/ABSTRACTS:

1) Pereira, E.F.R., Crista, C., Randall, W.R., and Albuquerque, E.X. Interactions between kynurenic acid and galantamine on α7 nicotinic receptors in hippocampal neurons. Abstr. Soc. Neurosci., #11419, 2003.

2) Popa R., Pereira E.F.R., Cintra, W.M., Maelicke, A., and Albuquerque, E.X. At clinically relevant concentrations galantaminone, a metabolite of galantamine, does not affect α7 nicotinic receptor activity in hippocampal neurons. Abstr. Soc. Neurosci., #9433, 2003.

3) Oliveira; M., Gary, T.M., Fawcett, W.P., Randall, W.R., Albuquerque, E.X., and Pereira, E.F.R. Neuroprotective effects of galantamine, a drug used to treat alzheimer's disease, in primary hippocampal cultures. Abstr. Soc. Neurosci. *(in press)* 2004.